PHYSICAL REVIEW B VOLUME 27, NUMBER 3 1 FEBRUARY 1983

Electronic structure of zirconium hydride: A proton NMR study

R. C. Bowman, Jr.*
Division of Chemistry and Chemical Engineering, California Institute of Technology, Pasadena, California 91125

E. L. Venturini
Sandia National Laboratories, Albuquerque, New Mexico 87185

B. D. Craft, A. Attalla, and D. B. Sullenger
Monsanto Research Corporation—Mound, Miamisburg, Ohio 45342
(Received 26 July 1982)

The proton spin-lattice relaxation times (T_1) and Knight shifts (σ_K) have been measured as a function of temperature in fcc (δ phase) and fct (ϵ phase) ZrH_x for hydrogen concentrations $1.5 \leq x \leq 2.0$. Interactions with the conduction electrons were found to be the only important T_1 relaxation processes below 320 K for the high-purity ZrH_x samples, and no anomalous temperature effects were observed between 320 and 100 K. The dominant hyperfine interaction for the protons was the transferred core-polarization term from the Zr d band. Both $(T_{1e}T)^{-1/2}$ and σ_K indicate that the density of electronic states $N(E_F)$ at the Fermi level is very dependent upon hydrogen content with a maximum occurring near $ZrH_{1.83}$. This behavior is ascribed to modifications in $N(E_F)$ through the fcc-fct distortion associated with a Jahn-Teller effect in the d bands. The proton NMR results are consistent with a recent band-theory calculation of fcc ZrH_2 and photoemission spectroscopy studies of ZrH_x when the changes in d bands caused by the Jahn-Teller tetragonal distortion are included. The fcc-fct distortions and electronic structures of the ZrH_x phases are compared with the corresponding properties of the TiH_x system.

I. INTRODUCTION

The electronic properties of the nonstoichiometric dihydrides formed by the group-IV*b* metals Ti, Zr, Hf, and some of their alloys have been the subjects of numerous theoretical[1–9] and experimental[10–26] studies. Understanding the formation and characteristics of the metal—hydrogen bonds in transition-metal hydrides has been a major motivating factor in most of this work. Much attention has also focused on the roles of temperature, hydrogen stoichiometry, and alloying on the face-centered-cubic— (fcc) to—face-centered-tetragonal (fct) distortions near the stoichiometric dihydride limit. The fcc-fct phase transitions have been associated[1,3,4,11,15–17,20,22,25,26] with a splitting of the energy bands at the Fermi level (E_F) that is analogous to the Jahn-Teller distortions[27] for the orbitally degenerate electronic energy levels in molecular systems. According to the Jahn-Teller model, the fcc-fct distortion is accompanied[4,11,25,26] by a decrease in $N(E_F)$, the density of electronic states at the Fermi level.

As described in the recent reviews by Switendick,[28,29] band-theory calculations of the electronic structures in various metal-hydrogen systems have clearly demonstrated the inadequacies of the historic "protonic" and the alternative "anionic" models that had been formulated using rigid-band concepts to describe metal-hydride electronic properties. According to the band-theory calculations for metal hydrides, interstitial hydrogen atoms interact strongly with metal bands of suitable symmetry[28,29] to form new hydrogen—metal bonding states[1–9] composed of the hybridized *s-d* levels and lying several eV below E_F of the host metal as well as other less significant changes in the d bands near E_F. Photoelectron spectroscopy measurements in group-IV*b* metal hydrides[18,22] have detected the presence of the hydrogen-bonding peaks in the valence-band levels that lie $\sim 5-7$ eV below E_F in semiquantitative agreement with the theoretical[1–9] band structures. A general feature of the calculated band structures

for the fcc dihydrides TiH_2 (Refs. 2, 3, 7, and 9) and ZrH_2 (Ref. 8) (the HfH_2 electronic structure has not yet been calculated) is E_F being very near (or on) the exact center of an extremely sharp peak in the density of states. It is the decrease in $N(E_F)$ with an accompanying small movement of E_F to a lower energy as the degeneracy is reduced for the lower symmetry that is the suggested[1,3,4,7] driving force for the fcc-fct distortion. In fact, reductions in $N(E_F)$ with an increase in the fct distortions are consistent with low-temperature specific heats,[11] photoelectron spectra,[22] and results from nuclear-magnetic-resonance (NMR) spectroscopy.[14–17,20,21,25,26] Experimental studies[14,25,30–32] of the nominal dihydrides $Ti_{1-y}M_yH_x$ where $M=$V, Nb, or Ta (i.e., group-V*b* metals with one more valence electron than Ti) and $1.9 \lesssim x \lesssim 2.0$ have indicated the fcc-fct phase transition is eliminated when $y \geq 0.15$. With a cautious assumption[1,8] of rigid-band behavior for the *d* bands near E_F, these observations imply that the extra electrons from the group-V*b* metals fill additional states to move the Fermi level above the sharp peak and thus stabilize the fcc phase since a Jahn-Teller splitting of the completely filled peak states cannot lower the energy. The changes in fcc-fct distortion behavior induced by varying the hydrogen concentration are more difficult to interpret[1,22,30,31] since band structure also changes with the hydrogen content, and a rigid-band description should not be rigorously valid. However, the fcc phases are stable when the hydrogen contents are sufficiently reduced to apparently shift E_F below the sharp peak.[1] No Jahn-Teller effect can occur if the degenerate states are either empty or filled.

Although the non-self-consistent band-theory calculations[1–4,7–9] for stoichiometric TiH_2 and ZrH_2 have provided a sound theoretical framework for the Jahn-Teller distortion mechanism, the absolute accuracies of the calculated energy levels and density of states are quite sensitive to initial atomic configurations, input values of the muffin-tin parameters, and the numerical procedures used during the actual computations. Hence, there are several quantitative differences among the calculated TiH_2 band structures[1–5,7,9] and with the experimental photoelectron energy distribution curves obtained by Weaver *et al.*[22] While these differences do not lessen confidence in the fundamental validity of the Jahn-Teller model for the fcc-fct distortions, detailed theoretical assessments of temperature and composition dependences have not yet been possible. Furthermore, the band calculations have not yet been extended to the substoichiometric hydrides and only limited results[1,4] are available for fct TiH_2.

The experimental situation is somewhat better, but there are still some serious limitations. For example, the room-temperature photoelectron spectra[22] of ZrH_x with $x=1.63$, 1.77, 1.86, and 1.94 do show changes in the band structure near E_F and about 7 eV below E_F that correlate with the fcc-fct distortion. However, the approximately 0.5-eV spectral resolution prevents more detailed observations of any smaller changes and the temperature behavior has not been studied using this technique. The composition behavior of the electronic specific heats[11] of TiH_x and ZrH_x indicate $N(E_F)$ is reduced by the fcc-fct distortions, but only a few samples were measured and these results pertain to temperatures below 10 K. Magnetic susceptibilities (χ) have been measured in TiH_x (Refs. 11 and 30) and $Ti_{1-y}M_yH_x$,[30–32] for $M=$V, Nb, Ta, and ZrH_x,[11,13] and have been related to the fcc-fct distortions and the temperature and composition dependences of $N(E_F)$. However, χ for transition metals usually has large-orbital (i.e., Van Vleck) contributions in addition to the Pauli terms that are directly proportional to $N(E_F)$. Hence, Switendick[28] has cautioned against assuming the χ changes only reflect variations in $N(E_F)$. NMR measurements of the Knight shifts (σ_K) and conduction-electron contributions to the spin-lattice relaxation times (T_1) usually monitor $N(E_F)$ through hyperfine interactions[33–36] at the nucleus. In fact, recent studies[14,15,25,26] of the proton σ_K and T_1 values in TiH_x, $Ti_{1-y}V_yH_x$, and $Ti_{1-y}Nb_yH_x$ have given temperature and composition behavior that is in excellent agreement with the $N(E_F)$ variations expected[1,4,7] for the TiH_x band structure and the Jahn-Teller distortions. Only limited proton NMR data[12,16,20] address the similar electronic properties for δ-phase (fcc) and ϵ-phase (fct) ZrH_x.

In the present study the temperature and composition dependences of the proton Knight shifts and spin-lattice relaxation times have been measured in high-purity polycrystalline ZrH_x for $1.5 \leq x \leq 2.0$. The purposes of this work are to provide some comprehensive conclusions on the electronic structures of δ- and ϵ-phase ZrH_x and to compare these results with recent theoretical predictions[1,2,7–9] and the similar proton NMR parameters[15,25] for the electronic structure of TiH_x. Analyses of the proton σ_K and T_1 data for the ZrH_x samples show the dominance of the transferred core-polarization hyperfine interaction[17,25,26] with the Zr *d* electrons at E_F and yield a composition-dependent maximum in $N(E_F)$ near $x=1.83$. These observations support the Jahn-Teller mechanism for the tetragonal distortion and are also consistent with recent augmented-plane-wave (APW) band-theory calculations[8] for fcc ZrH_2 and the photoemission[18,22] and soft x-ray emission[19] spectra for ZrH_x as well as an electron-spin-resonance study[24] of Er impurities in ZrH_x.

II. A BRIEF REVIEW OF SOME ZrH_x PROPERTIES

The phase diagram and physical properties of the zirconium-hydrogen system have been extensively studied.[37] The several ZrH_x phases[37] are typical metallic solids with no unusual electrical properties[38] and normal paramagnetic behavior[11,13] for a transition-metal alloy if ferromagnetic impurities[11,13] are avoided. For $x \geq 1.50$ and temperatures below 700 K, the cubic (fcc) δ-phase and tetragonal (fct) ϵ-phase are the only known stable ZrH_x phases. A presumably metastable[39–41] γ-phase monohydride with a tetragonal crystal structure[42] coexists with the δ phase for $x \lesssim 1.5-1.6$. Naskidashvili and coworkers[43–45] have reported some low-temperature (i.e., $T < 200$ K) phase transitions for ZrH_x with $1.65 \leq x \leq 1.85$, but there have been no confirmations for these transitions by other groups.[24,46,47] The structures of the γ, δ, and ϵ phases have been established by x-ray and neutron diffraction[37,42,48,49] where the hydrogen atoms only occupy tetrahedral interstitial sites for each phase.[42,46] However, the phase boundaries for the δ and ϵ phases have not been completely resolved[11,24,37,39,49] and contradictory behavior has been observed[39–42,46] for the γ phase. With the use of results taken from several sources (including present x-ray diffraction measurements on high-purity ZrH_x samples), the single-phase region for cubic δ-phase ZrH_x is $1.55(5) \leq x \leq 1.65(2)$ from above 300 K to much lower temperatures (i.e., $\lesssim 200$ K), while the single-phase region for tetragonal ϵ-phase ZrH_x is $1.74(2) \leq x \leq 2.0$ over a similar temperature range. A mixed δ- and ϵ-phase region exists for $1.65(2) \leq x \leq 1.74(2)$ while γ-phase $ZrH_{1.0}$ as well as the hcp Zr-metal α phase are found[37,39–42] when $x \leq 1.55(5)$.

The ZrH_x phases are thermodynamically quite stable with very low dissociation pressures[37] at temperatures below 500 K. Because massive ZrH_x can be handled in air at room temperature without an apparent loss in stoichiometry, ZrH_x has often been assumed[37] rather unreactive to oxygen or water vapor. However, clean surfaces of zirconium metal and hydride have been observed[18] to rapidly form ZrO_2 films from the residual oxygen in a vacuum at the low 10^{-9}-Torr range. The oxide film serves as a passivating layer which inhibits further reaction at ambient temperature. In massive samples only a relatively small quantity of Zr will be converted to the oxide and no significant reduction in hydrogen content is usually detected. However, fine powders of ZrH_x should be prepared and handled only in vacuum or inert-atmosphere environments to avoid excessive oxidation.

Gupta and Burger[8] have, apparently, performed the most complete non-self-consistent one-electron band calculation of the electronic structure for fcc $ZrH_{2.0}$. Figure 1 reproduces their theoretical total density of states where several features should be noted. First, the hydrogen—metal bonding states are split with peaks ~ 6 and ~ 7 eV below E_F. This reflects a bonding-antibonding effect[28,29] between the two hydrogen atoms. The Fermi level falls exactly at the center of a very sharp peak in $N(E)$ which rises out of a nearly flat plateau (actually, a slightly decreasing density is found in the region below the peak). Finally, the metal-hydrogen peak is nearly completely separated from the higher d bands. The experimental photoelectron energy distribution curves[22] for fcc δ-phase $ZrH_{1.63}$ and fct ϵ-phase $ZrH_{1.94}$ are in excellent qualitative agreement with Fig. 1 although the experimental peaks in the presumed metal—hydrogen bonding region are only partially resolved and differ by about 1 eV from the calculated peak positions.[8] However, both E_F and the detailed shape of the $N(E)$ curve will change as the hydrogen concentration is decreased (i.e., in fcc δ phase), and as the lattice is distorted in the fct ϵ phase (i.e., the Jahn-Teller splitting of the sharp peak at E_F in Fig. 1). Hence, quantitative agreement with Fig. 1 should not be expected, but all of the major predicted properties[8] have been observed by Weaver *et al.*[22]

Since Ti and Zr have the same valency, the electronic properties and structures of the fcc and fct ZrH_x phases are very similar to those for the TiH_x system.[1–4,7,9] However, the several minor differences in the photoelectron-emission spectra[22] indicate the $N(E)$ curves are clearly not identical for TiH_x and ZrH_x. Furthermore, Gupta's calcula-

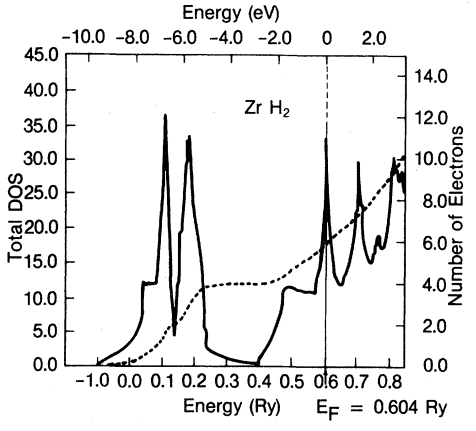

FIG. 1. Total density of states (DOS) of fcc ZrH_2 as calculated by Gupta and Burger. DOS given by solid line curve and left-hand-side scale with units of states of both spin per rydberg unit cell. Number of valence electrons given by dashed line and right-hand-side scale.

tions[7,8] and several experimental studies[11,12,15,16,20,21] show that $N(E_F)$ values for ZrH_x are significantly smaller than the corresponding $N(E_F)$ values obtained for TiH_x samples with similar compositions. This may be at least partially attributed to the larger unit-cell volumes[11] for the ZrH_x phases relative to corresponding TiH_x samples. There should be smaller metal-hydrogen overlap and metal-metal overlaps for the more diffuse $4d$ orbitals of Zr atoms compared to the corresponding overlaps for the $3d$ orbitals of the Ti atoms. Finally, the magnitudes of the fcc-fct distortions arising from the Jahn-Teller effect in the electronic energy bands are much greater for the ZrH_x system. The highest temperature for the existence of tetragonal $TiH_{2.0}$ is about 310 K with the fcc-fct transition temperature occurring at lower temperatures as the stoichiometry is decreased.[11,15,30,31,48] However, tetragonal ϵ-phase ZrH_x is the stable room-temperature phase for $x \geq 1.74$, and $ZrH_{1.92}$ remains tetragonal up to temperature above 750 K according to Yakel.[48] Nevertheless, any differences in fcc-fct behavior are more a matter of degree since the same basic mechanism is believed[22] responsible in all the group-IV metal hydrides.

III. EXPERIMENTAL DETAILS

The ZrH_x samples were prepared by direct reaction between zone-refined Zr metal foils[50] and hydrogen gas that had been purified by diffusion through a Pd-Ag tube. The synthesis procedures have been previously described[47] and compositions between 1.50 and 2.00 were obtained where the volumetric analyses of absorbed hydrogen and weight gains usually agreed within $x = \pm 0.01$. The few discrepancies were resolved using volumetric analyses of hydrogen evolution during thermal desorption from portions of the samples. The ZrH_x foils were ground under a purified argon atmosphere to produce powders[47] that were subsequently sealed in evacuated glass tubes for the NMR experiments.

X-ray diffraction measurements using standard Debye-Scherrer photographic techniques to record the powder patterns were performed at room temperature on every ZrH_x sample. A small amount of γ-phase ZrH was detected in $ZrH_{1.50}$ while only the strongest γ-phase line was found (as a very weak line) in $ZrH_{1.55}$. The powder pattern for $ZrH_{1.70}$ gave approximately equal amounts of the δ and ϵ phases. All of the other ZrH_x samples were single phase within the detection limits of the x-ray diffraction method. Figure 2 gives the room-temperature lattice parameters for the ZrH_x samples with $x \geq 1.50$ and the corresponding phase boundaries. The lattice parameters in Fig. 2 are generally

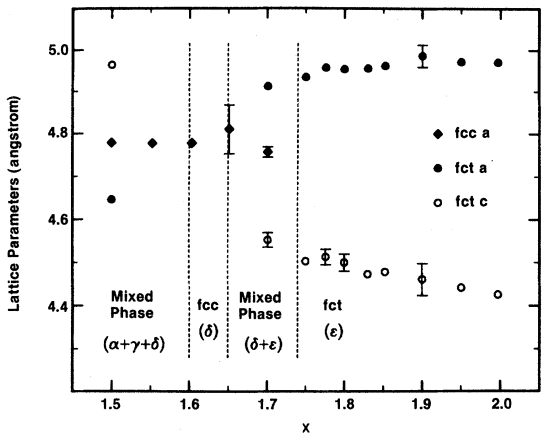

FIG. 2. Room-temperature lattice parameters for high-purity ZrH_x where phase boundaries are based upon several literature sources (i.e., Refs. 24, 39—42, and 49).

in very good agreement with values for ZrH_x from several previous measurements by others.[11,22,39,49]

Wide-band transient spectrometers were used for all the NMR experiments. The proton spin-lattice relaxation times (T_1) were obtained by the standard inversion-recovery method at a resonance frequency of 34.5 MHz. Within experimental uncertainties the magnetization recoveries were exponential and yielded T_1 values with an average precision of $\pm 3\%$ over the temperature range 100—300 K. The proton Knight shifts were measured in four ZrH_x samples with the multiple-phase zero-crossing method of Burum *et al.*[51] on a spectrometer where the magnetic field was locked by an external-probe system and the nominal proton resonance frequency was 56.4 MHz. The σ_K values are relative to an external reference of tetramethylsilane (TMS) contained in a spherical bulb and have an experimental precision of ± 2 ppm over the temperature range 170—310 K. No corrections to the σ_K values for the demagnetization effects[35] due to sample susceptibility have been made since the χ values for high-purity ZrH_x should be sufficiently small[11,13] to make relatively minor contributions of about 5 ppm to the total proton shifts.

IV. RESULTS

Figures 3 and 4 show the temperature-dependent behavior of the proton T_1 values for several ZrH_x samples. There is no indication for any anomalous breaks from the smooth T_1 increases as the temperature is lowered below 200 K for any of the high-purity ZrH_x samples. This contrasts with the low-temperature anomalies in proton T_1 that were reported by Naskidashvili *et al.*[44] for $ZrH_{1.65}$ and $ZrH_{1.75}$ which they associated with possible phase

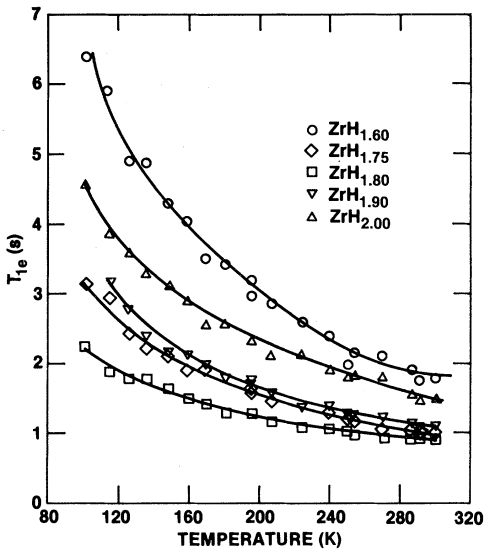

FIG. 3. Temperature dependence of proton spin-lattice relaxation times for some ZrH_x samples. Curves through data points are merely visual aids.

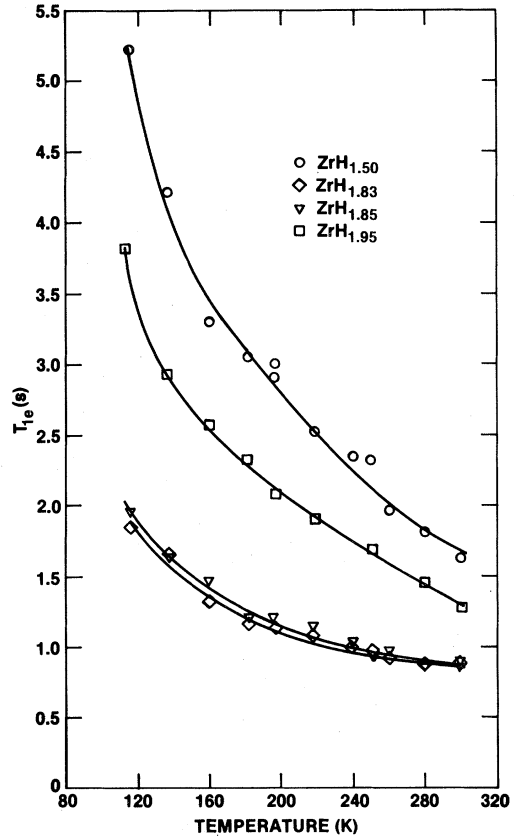

FIG. 4. Temperature dependence of proton spin-lattice relaxation times for more ZrH_x samples. Curves are merely visual aids.

transitions implied by other techniques.[43,45] However, from neutron-diffraction studies, Petrunin *et al.*[46] saw no changes in the phase composition of $ZrD_{1.82}$ when it was cooled to liquid-nitrogen temperature. Furthermore, no evidence for these low-temperature phase transitions was found from electron-spin-resonance (ESR) studies[24] of Er ions in ZrH_x or low-temperature proton line-shape measurements[47] on high-purity ZrH_x samples. Petrunin *et al.*[46] have suggested that the low-temperatures anomalies[43–45] may actually involve transitions of an impurity phase. Since no anomalies are found for the T_1 data in Figs. 3 and 4 for high-purity ZrH_x samples, there is again no confirmation for low-temperature phase transitions in ZrH_x as proposed by Naskidashvili *et al.*[43–45] Hence their existence remains unsubstantiated and must be regarded as highly speculative and will not be considered further.

In general, the total relaxation rate T_1^{-1} in a metallic solid can be separated into three potential contributions,

$$\frac{1}{T_1}=\frac{1}{T_{1e}}+\frac{1}{T_{1d}}+\frac{1}{T_{1p}}\ , \tag{1}$$

where T_{1e} represents relaxation due to hyperfine interactions[33–36] with the conduction electrons, T_{1d} is the well-known[36] diffusion contribution, and T_{1p} is the relaxation term for localized paramagnetic centers. The rigid-lattice dipolar line shapes for proton NMR spectra[47] of polycrystalline ZrH_x at room temperature as well as previous proton T_1 measurements[16,20,21] imply that T_{1d} is not a significant contribution to the proton spin-lattice relaxation process until the temperature exceeds at least 400 K. Hence, the diffusion contributions to all the T_1 data in Figs. 3 and 4 will be completely negligible. The temperature-independent T_{1p} term can also be neglected since the concentration of any paramagnetic impurities is very low in these high-purity ZrH_x samples. Thus, the experimental T_1 values of Figs. 3 and 4 only correspond to the conduction-electron relaxation time T_{1e}. The anomalously short proton T_1 data of Khodosov and Shepilov[12] for ZrH_x, which are nearly a factor of 10 shorter than the T_1 values in Figs. 3 and 4, probably contain large T_{1p} contributions although this cannot be directly established since the purities of their samples are unknown. It should be noted that Khodosov and Shepilov[12] also gave proton T_1 values for TiH_x samples that are much shorter than the spin-lattice relaxation times obtained for TiH_x by other research groups.[15,21,25,26] Hence, the proton T_1 data of Khodosov and Shepilov[12] for ZrH_x and TiH_x are probably not reliable indicators of the conduction-

electron contributions to spin-lattice relaxation times.

The temperature dependence of the proton Knight shifts σ_K were measured for $ZrH_{1.60}$, $ZrH_{1.80}$, $ZrH_{1.90}$, and $ZrH_{2.00}$. These results are summarized in Fig. 5 where the σ_K values are negative (i.e., the shifts are upfield for a constant frequency) relative to the resonance frequency for the external standard of TMS. In some previous studies[52–54] of the proton Knight shifts for metal hydrides, the frequency of the bare proton nucleus (i.e., H^+) has been chosen as the reference. This choice may have been biased by use of the rigid-band proton model[28] to describe NMR results[36] in the hydrides. However, photoemission[18,22] and soft x-ray emission[19] spectroscopy, as well as band-theory calculations, clearly indicate an increased electron density about the hydrogen interstitials in ZrH_x. Hence, it is probably more appropriate to reference the proton Knight shift to the frequency for the hydride anion (i.e., H^-) rather than H^+. According to Mason[55] the chemical shift for free H^- is 27 ppm upfield from the H^+ reference. The measurements of Nicol and Vaughan[56] on proton shifts in the alkaline hydrides CaH_2, SrH_2, and BaH_2 imply an average upfield chemical shift of 23 ± 2 ppm for the hydride ion relative to H^+. A similar chemical shift is also expected for hydrogen interstitials in the transition metals, but it is impossible to uniquely define an absolute value. Consequently, the proton σ_K values are referenced to TMS which is about 30 ppm upfield from the bare proton frequency. The use of TMS as the reference may give an absolute uncertainty in σ_K of $\pm5-10$ ppm, but at least a consistent estimate of the chemical shift term has been included.

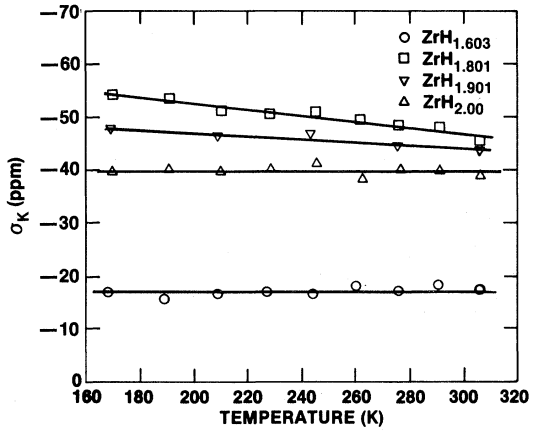

FIG. 5. Proton Knight shifts for polycrystalline ZrH_x measured using the multiple-pulse zero-crossing technique of Ref. 51 at a resonance frequency of 56.4 MHz and referenced to an external standard of TMS.

V. DISCUSSION

A. Hyperfine interactions of protons in ZrH_x

The nuclear spin systems in metals are affected by the electronic structure of the metal through the hyperfine fields produced by the conduction electrons at the sites of the nuclei. In transition metals and alloys, including the metal hydrides, the conduction electrons will primarily occupy the s and d orbitals of the constituent atoms. However, the densities of d-electron states in the region of the Fermi level are usually much larger than the densities of the s-electron states since E_F lies in the rather narrow d band formed by the transition-metal orbitals while the s band extends over a wide energy distribution. Although detailed models[33–35] have been formulated for the hyperfine interactions in the simple metals, the general expressions are rarely applied to transition-metal systems since unique identification of the various hyperfine interactions is usually impossible. Instead, some simpler models that neglect effects from electron-electron correlation, mixing of the s and d bands, and various higher-order contributions have been extensively used[33–36] to analyze Knight shifts and T_{1e} parameters for transition metals and transition-metal alloys. Within the free-electron approximation and assuming only s and d orbitals contribute to the hyperfine interactions, the Knight shift and T_{1e} value can each be separated into three components,

$$\sigma_K = 2\mu_B[H_{\rm hf}(s)N_s(E_F)+H_{\rm hf}(d)N_d(E_F)] + \left[\frac{1}{N_A\mu_B}\right]H'_{\rm hf}(o)\chi_0 , \quad (2)$$

$$\frac{1}{T_{1e}T} = 4\pi\hbar\gamma_I^2 k_B\{[H_{\rm hf}(s)N_s(E_F)]^2 + [H_{\rm hf}(d)N_d(E_F)]^2 q + [H_{\rm hf}(o)N_d(E_F)]^2 p\} . \quad (3)$$

Here, μ_B is the Bohr magneton, N_A is Avogrado's number, $\hbar$ is Planck's constant, γ_I is the gyromagnetic ratio for nuclei with quantum number I, k_B is the Boltzmann's constant, $N_s(E_F)$ and $N_d(E_F)$ are the s- and d-band densities of states at the Fermi level, respectively, χ_0 is the Van Vleck term of the magnetic susceptibility caused by paramagnetic orbital interactions[33] with the d electrons, and p and q are the reduction factors resulting from d-electron orbital degeneracy at E_F as described by Narath.[33] The hyperfine fields at the nuclei are produced as follows: $H_{\rm hf}(s)$ is due to the Fermi-contact interac-

tion with unpaired s electrons at E_F, $H_{hf}(d)$ is the "core" polarization of spin-paired s orbitals at energies below E_F by the unpaired d electrons at E_F, and $H_{hf}(o)$ and $H'_{hf}(o)$ are the fields generated by the orbital motion of the d electrons. Although $H_{hf}(o)$ represents only d electrons at E_F, $H'_{hf}(o)$ is an average[33] over all contributing states in the d band lying above and below E_F. Since theoretical estimates of the orbital fields are very difficult,[34] the approximation $H_{hf}(o) \approx H'_{hf}(o)$ is often used to analyze experimental data. Although the contact field $H_{hf}(s)$ is usually much larger[35] than the core-polarization or orbital hyperfine fields, the large $N_d(E_F)$ in most transition-metal systems usually ensures that core-polarization and/or orbital terms will dominate T_{1e} and σ_K. Although $H_{hf}(s)$ is always positive,[33–35] $H_{hf}(d)$ is negative[33] for the transition metals. Hence, significant cancellations can occur in σ_K to give positive, negative, or even zero shifts depending upon the relative magnitudes of the three terms in Eq. (2). Since only the squares of the hyperfine fields influence $(T_{1e}T)^{-1}$, the three terms in Eq. (3) are always additive.

Because several independent parameters contribute to the σ_K and $(T_{1e}T)^{-1}$ values for transition-metal systems, quantitative assessments of the individual hyperfine fields and density of states are usually very difficult without supplemental experimental and theoretical results. Nevertheless, many significant insights on the electron structures of transition metals have been obtained from the σ_K and $(T_{1e}T)^{-1}$ data[33–35] without explicitly evaluating all of the parameters in Eqs. (2) and (3). If one of the terms dominates Eq. (3), $(T_{1e}T)^{-1/2}$ is directly proportional to the density of states at E_F. When either the Fermi-contact or core-polarization hyperfine interaction is dominant, both σ_K and $(T_{1e}T)^{-1/2}$ will directly correspond to $N_s(E_F)$ or $N_d(E_F)$, respectively, and the NMR parameters will exhibit very similar behavior when temperature or alloy composition is varied. Because the orbital terms $H'_{hf}(o)$ and χ_0 for σ_K in Eq. (2) depend upon averages over the entire d band,[34,35] the orbital term is not proportional to $N_d(E_F)$ and usually gives a temperature-independent contribution to σ_K. However, the orbital contribution to $(T_{1e}T)^{-1/2}$ is directly proportional to $N_d(E_F)$ and will usually exhibit a large variation with temperature whenever E_F occurs in or near a peak in the density of states. Hence, significant differences in temperature behavior for σ_K and $(T_{1e}T)^{-1/2}$ are expected whenever orbital contributions are large and E_F falls near a peak in the density of states. The orbital contributions are generally large for the transition-metal nuclei[33–35] and give positive contributions to σ_K as were observed[10] for Ti nuclei in TiH_x with $1.7 \leq x \leq 2.0$.

Because the hyperfine field from the hydrogen 1s orbital is intrinsically small, transferred hyperfine interactions from the metal d states are assumed[15–17,25,26] to be the major contributors to the proton Knight shifts and T_{1e} relaxation times. In fact, the transition-metal d states appear to dominate the hyperfine interactions for any non-transition-element nucleus[57–60] that is contained in a transition-metal host. In his analysis of the electronic structure of TiH_x, Korn[15] proposed a transferred orbital hyperfine interaction for protons. His major justification was that the proton shifts of Stalinski *et al.*[61] did not show the same stoichiometry dependence as Korn's proton $(T_{1e}T)^{-1/2}$ data. This difference is consistent with the behavior expected[33] for orbital hyperfine interactions. However, the proton Knight shifts of Stalinski *et al.*[61] were obtained by cw-NMR techniques and are very imprecise since the shifts are much smaller than the dipolar linewidths. More reliable proton σ_K values for TiH_x were recently obtained by multiple-pulse techniques[26] and gave excellent agreement with both the composition and temperature dependencies of the proton $(T_{1e}T)^{-1/2}$ values.[15,26] Similar agreement between σ_k and $(T_{1e}T)^{-1/2}$ behavior has been obtained[25] for protons in $Ti_{1-y}V_yH_{1.95}$. Hence, the original experimental basis for Korn's proposed orbital hyperfine interactions at the proton sites has been invalidated by subsequent (and more accurate) proton σ_K measurements.[25,26] Furthermore, there is experimental and theoretical evidence[57–60] that orbital contributions are usually negligible for non-transition-metal nuclei in transition-metal hosts.

The recent NMR data for TiH_x and related alloy hydrides[17,25,26] favor the dominance of a "transferred" core-polarization hyperfine interaction from the metal d orbitals to the filled hydrogen 1s orbitals lying below E_F. This interpretation is consistent with the band-theory calculations[1–4,7,9] which have indicated the formation of the s-d hybridized metal–hydrogen bonding band. The negative proton σ_K values[17,25,26,61] are easily associated with core-polarization interactions.[33–35,57–60] In contrast the orbital hyperfine interaction usually gives positive Knight shifts and tenuous arguments were required to rationalize[15] the negative-proton σ_K values in TiH_x. Since the valence bands of Ti and Zr are isoelectronic and the proton σ_K in ZrH_x are also negative as shown in Fig. 5, any orbital contributions to the proton hyperfine interactions will be neglected during the remaining discussion. Hence, the experimental proton σ_K and $(T_{1e}T)^{-1/2}$ parameters for ZrH_x are assumed proportional to the density of electron states at E_F through the Fermi-contact and core-polarization terms as shown in

Eqs. (2) and (3).

A useful relationship that was originally derived by Korringa[62] for the contact hyperfine interaction can be generalized in the form

$$q_{\text{expt}} = C_K / \sigma_K^2 T_{1e} T \ , \tag{4}$$

where

$$C_K = \hbar \gamma_e^2 / (4\pi k_B \gamma_I^2)$$

and γ_e is the electron gyromagnetic ratio. When the Fermi-contact terms dominate both σ_K and T_{1e}, $q_{\text{expt}} = 1.0$ if the electron-electron interactions[33] are excluded. For the core-polarization terms, $q_{\text{expt}} = q$, the reduction factor for T_{1e} relaxation by d electrons. In cubic lattices, q obeys[33]

$$q = \tfrac{1}{3} f^2(t_{2g}) + \tfrac{1}{2}[1 - f(t_{2g})]^2 \ , \tag{5}$$

where $f(t_{2g})$ is the fractional character of the t_{2g} d orbitals at the Fermi surface. The minimum value for q is 0.20 when $f(t_{2g}) = \frac{3}{5}$ and there is an equal population of all five d orbitals at the Fermi level. The maxima for q are 0.50 and 0.33 when $f(t_{2g})$ equals zero or one, respectively. However, $q_{\text{expt}} > 0.5$ are possible if both contact and core-polarization interactions contribute to σ_K because of the fortuitous cancellations of positive and negative shift contributions. In noncubic lattices q will not be given by Eq. (5), but the $\sim 10\%$ tetragonal distortion in ϵ-phase ZrH_x should not lead to large deviations and $0.2 \lesssim q \lesssim 0.5$ should remain approximately valid for the core-polarization interaction.

The shift in the Fermi level and the widening of the electron distribution function about this level with increasing temperature can make σ_K and T_{1e} temperature dependent if E_F happens to lie in a region where the density of states is very dependent upon energy. This temperature dependence will be given by the expressions[15,26,63]

$$\sigma_K(T) = \sigma_K(0) \left\{ 1 + \tfrac{1}{6}\pi^2 k_B^2 T^2 \left[\frac{1}{N(E)} \frac{d^2 N(E)}{dE^2} - \left[\frac{1}{N(E)} \frac{dN(E)}{dE} \right]^2 \right]_{E=E_F} \right\} , \tag{6}$$

$$\frac{1}{T_{1e}(T)T} = \frac{1}{T_{1e}(0)T} \left[1 + \tfrac{1}{3}\pi^2 k_B^2 T^2 \left[\frac{1}{N(E)} \frac{d^2 N(E)}{dE^2} \right] \right]_{E=E_F} . \tag{7}$$

Since $\sigma_K(T)$ depends on the difference between the first and second derivatives of $N(E)$, $\sigma_K(T)$ will not necessarily exhibit the same temperature behavior as $[T_{1e}(T)T]^{-1}$. In fact, $\sigma_K(T)$ could have an opposite dependence or be temperature independent when $[T_{1e}(T)T]^{-1}$ varies with temperature. According to Eqs. (6) and (7), the major factor determining σ_K and $(T_{1e}T)^{-1}$ temperature-dependent behavior is the relative position of E_F to a peak. However, a second mechanism can also produce temperature-dependent σ_K and $(T_{1e}T)^{-1/2}$ values. If $N(E_F)$ itself is strongly temperature dependent due to a change in some external parameter (e.g., an increasing tetragonal distortion from the Jahn-Teller effect), σ_K and $T_{1e}T$ will directly follow the change in $N(E_F)$ and changes associated with Eqs. (6) and (7) probably make only secondary contributions. The reduction in $N_d(E_F)$ for TiH_2 below 310 K is presumably responsible[25,26] for the temperature behavior of the proton σ_K and $(T_{1e}T)^{-1/2}$ parameters in TiH_x when $x \gtrsim 1.8$. In the next section it will be shown that a different situation apparently causes σ_K and $(T_{1e}T^{-1/2})$ to be temperature dependent in ϵ-phase ZrH_x [i.e., the processes corresponding to Eqs. (6) and (7) are responsible].

B. Relation of proton NMR parameters to fct distortion and electronic structure in ZrH_x

Figures 6 and 7 show the temperature-dependent behavior of the proton $(T_{1e}T)^{-1/2}$ values for the T_1 data presented in Figs. 3 and 4, respectively. From the discussion of the preceding section, $(T_{1e}T)^{-1/2}$ is presumed directly proportional to the local density of electron states at the Fermi level as sampled at the proton site. The proton Knight shifts are also proportional to $N(E_F)$. The negative σ_K values in Fig. 5 indicate the dominance of the transferred core-polarization hyperfine interactions over the Fermi-contact contribution as has been previously concluded for protons in the Ti-based dihydrides.[17,25,26] This implies $N_d(E_F) \gg N_s(E_F)$ in all these hydrides which is completely consistent with the band-theory calculations for TiH_2 (Refs. 1–4, 7, and 9) and ZrH_2.[8] Hence, $(T_{1e}T)^{-1/2}$ should also mainly represent $N_d(E_F)$ through the core-polarization interactions. However, some contributions from the contact term are expected for both σ_K and $(T_{1e}T)^{-1/2}$ since $N_s(E_F)$ is predicted[8] to be finite (although small) in fcc ZrH_2 and $H_{\text{hf}}(s)$ should be larger[35] than $|H_{\text{hf}}(d)|$.

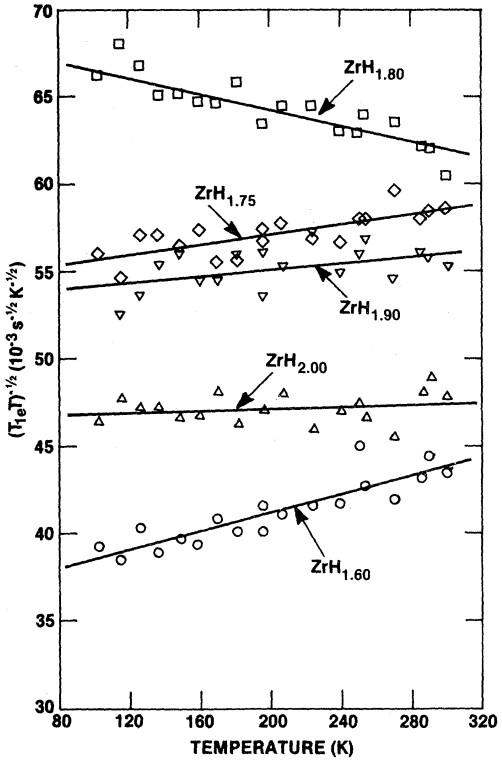

FIG. 6. Temperature dependence of proton $(T_{1e}T)^{-1/2}$ for the ZrH_x samples given in Fig. 3. Straight lines are linear least-squares fits to the data.

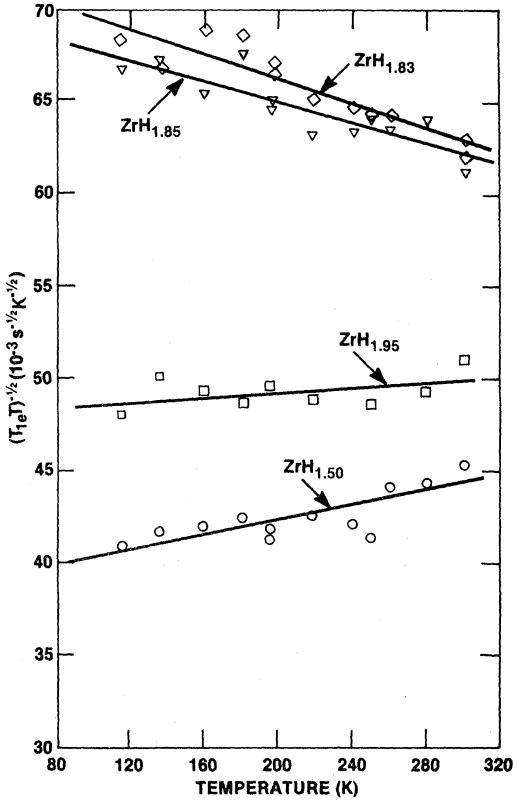

FIG. 7. Temperature dependence of proton $(T_{1e}T)^{-1/2}$ for the ZrH_x samples given in Fig. 4. Straight lines are linear least-squares fits to the data.

The composition dependence of the proton σ_K and $(T_{1e}T)^{-1/2}$ parameters in ZrH_x is summarized in Fig. 8 for various temperatures. The major feature for $(T_{1e}T)^{-1/2}$ is an increase above $x=1.75$ (i.e., in the ϵ-phase) to reach a maximum near $x=1.83$ before decreasing smoothly with composition to $x=2.00$. $(T_{1e}T)^{-1/2}$ exhibits the largest temperature effects for $1.80 \leq x \leq 1.85$ (i.e., at the peak). Similar behavior is also noted for the proton σ_K; however, neither the composition nor temperature dependence of σ_K is quite as large as seen for $(T_{1e}T)^{-1/2}$.

Korn[16] has reported preliminary measurements of the room-temperature variation of proton $(T_{1e}T)^{-1/2}$ as a function of hydrogen concentration for ZrH_x with $1.54 \leq x \leq 2.00$. His $(T_{1e}T)^{-1/2}$ data also showed a large peak near $x=1.82$ in excellent agreement with Fig. 8. However, Korn's $(T_{1e}T)^{-1/2}$ values are consistently 10–15% larger than the present results and Korn found $(T_{1e}T)^{-1/2}$ to increase by about 10% in the composition range $1.54 \leq x < 1.64$ (i.e., in the mixed $\gamma+\delta$ and pure δ-phase regions), while Fig. 8 indicates $(T_{1e}T)^{-1/2}$ at room temperature is essentially independent of com-

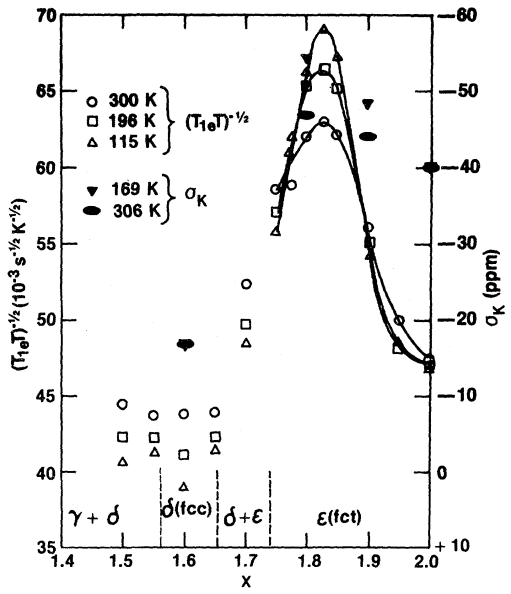

FIG. 8. Composition dependence of proton $(T_{1e}T)^{-1/2}$ and σ_K parameters for various temperatures.

position for $1.50 \leq x \leq 1.65$, which is in better accord with the ZrH_x phase diagrams.[37,39–42] Finally, Korn reports a $(T_{1e}T)^{-1/2}$ minimum in the $\delta+\epsilon$ mixed phase near $x=1.72$ that is not apparent in Fig. 8. Since Korn's paper[16] is brief, there is not enough information to resolve these discrepancies with the present data in Fig. 8 although his systematically larger $(T_{1e}T)^{-1/2}$ values may represent paramagnetic T_{1p} contributions to the spin-lattice relaxation times. Nevertheless, a well-defined $(T_{1e}T)^{-1/2}$ peak in the fct ϵ-phase region seems to be an unmistakeable property of ZrH_x since it was so clearly present in both studies. This feature should be associated with changes in $N(E_F)$ as the hydrogen concentration is varied.

In order to obtain a better understanding of the proton hyperfine interactions and the character of electron states at E_F, the generalized Korringa relation of Eq. (4) was applied on the samples $ZrH_{1.60}$, $ZrH_{1.80}$, $ZrH_{1.90}$, and $ZrH_{2.00}$. The resulting parameters q_{expt} at 300 and 170 K are summarized in Table I. Because the proton σ_K shifts for ZrH_x are small, their absolute values have rather large uncertainties due to choice of a zero-shift reference (i.e., the TMS frequency) and the neglect of possible susceptibility corrections.[25,26,35] Hence, the q_{expt} values in Table I have limited accuracy and should not be regarded as definitive in deducing the relative proportions of s and d electron character at E_F. However, more qualitative interpretations of q_{expt} should be fairly reliable. For example, there is probably an appreciable mixture of Fermi-contact and core-polarization contributions for $ZrH_{1.60}$ since $q_{\text{expt}} > 1.0$. While the negative σ_K implies $N_d(E_F) > N_s(E_F)$ for $ZrH_{1.60}$, a more quantitative estimate of $N_s(E_F)$ and $N_d(E_F)$ is not possible since the relevant hyperfine fields $H_{\text{hf}}(s)$ and $H_{\text{hf}}(d)$ are unknown. The q_{expt} values for the three ϵ-phase samples with $x \geq 1.80$ are within the range expected[33] for the core-polarization reduction factor (i.e., $0.2 \leq q \leq 0.5$ for a cubic lattice). However, the tetragonal distortion (i.e., $c/a \approx 0.9$) in ϵ-phase ZrH_x may influence the allowed range since the orbital degeneracy of the d functions will change as the symmetry is reduced by the distortion. Furthermore, some residual contact contribution from s states at E_F could also be present, but this term must be much less than for the δ phase since $q_{\text{expt}} < 0.5$ for the ϵ-phase samples. Hence, $N_d(E_F)$ is probably much larger than $N_s(E_F)$ for fct ϵ-phase ZrH_x, and E_F has moved further up into the d bands as the hydrogen concentration is increased. This trend is consistent with the general predictions[28,29] of the theoretical band-structure calculations.

Table I also includes mean slopes of the temperature behavior of the proton σ_K and $(T_{1e}T)^{-1}$ parameters for several ZrH_x samples. Although positive or near-zero slopes are observed when $x < 1.8$ or $x > 1.9$, the proton parameters for the samples with $1.80 \leq x \leq 1.85$ have strongly negative temperature dependence as shown in Figs. 5–8 and Table I. Assuming the temperature dependence corresponds to the thermal-broadening effects of the electron distribution functions, Eqs. (6) and (7) can approximately relate the slopes of σ_K and $(T_{1e}T)^{-1}$ in Table I to the derivatives at E_F for the density of states with respect to electron energy. Since both σ_K and $(T_{1e}T)^{-1}$ have negative temperature slopes near $x=1.83$, E_F must fall on a local maximum in the density of states at this composition. On the other hand, nearly flat (or, at least, more slowly changing functions with convex curvatures) density of states are indicated for the δ phase and $x > 1.90$. This description of the ZrH_x density of states is not very consistent with the calculated[8] one shown in Fig. 1 for fcc ZrH_2 if a quasi-rigid-band model is used to shift E_F to lower energies as the ZrH_x stoichiometry is decreased. However, ϵ-phase ZrH_x is fct and the Jahn-Teller mechanism[1,4] predicts the energy levels responsible for the $N(E_F)$ peak in fcc ZrH_2 to split during the tetragonal distortion.

TABLE I. Korringa parameters and slopes for temperature dependences of σ_K and $(T_{1e}T)^{-1}$ for ZrH_x samples.

Sample	c/a ratio	q_{expt} 300 K	q_{expt} 170 K	Slope σ_K (ppm/deg)	Slope $(T_{1e}T)^{-1/2}$ (10^{-4} $s^{-1}K^{-1}$/deg)
δ-$ZrH_{1.60}$	1.000	1.73	1.47	~0	+0.022
ϵ-$ZrH_{1.75}$	0.913				+0.017
ϵ-$ZrH_{1.80}$	0.908	0.46	0.38	−0.053	−0.029
ϵ-$ZrH_{1.85}$	0.902				−0.047
ϵ-$ZrH_{1.90}$	0.895	0.43	0.35	−0.031	+0.010
ϵ-$ZrH_{1.95}$	0.893				+0.008
ϵ-$ZrH_{2.00}$	0.890	0.37	0.37	~0	+0.003

Schematic pictures of the density of states of the d bands in the region near E_F for fcc δ-phase ZrH_x and fct ϵ-phase ZrH_x are given in Fig. 9. The calculated curves by Gupta and Burger[8] serve as the basis for $N(E)$ in the fcc structure while the composition dependence of the proton $(T_{1e}T)^{-1/2}$ data and the presumably symmetric band splitting from the Jahn-Teller effect leads to the proposed density-of-states shape for the tetragonal structure. A quasi-rigid-band model, which recognizes that some electrons associated with the hydrogen atoms will go into the metal–hydrogen bonding states[1,28,29] lying several eV below E_F, has been used to locate the Fermi levels at several ZrH_x compositions. The magnitude of the splitting between the two peaks for ϵ-phase ZrH_x will probably be sensitive to the c/a ratio as well as some secondary perturbations with changes in hydrogen concentrations since the rigid band cannot be rigorously valid.[7,8] However, the c/a ratio only changes from 0.91 to 0.89 over the composition range $1.75 \leq x \leq 2.00$ which is small compared to the 10% distortion that characterizes the ϵ phase. Hence, the increase of the Jahn-Teller splitting in ϵ-phase ZrH_x with increasing x should not be a large effect, but it could contribute (along with the electrons supplied by the hydrogen atoms) to accelerate the rise of E_F through the low-energy peak in $N(E)$ towards a presumably rather flat valley at $x=2.00$.

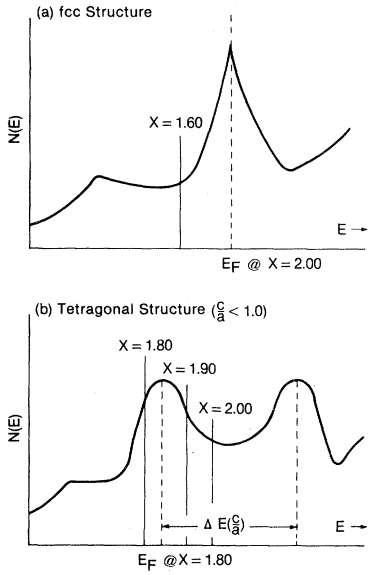

FIG. 9. (a) Schematic densities of states of d bands for fcc and (b) fct ZrH_x. Solid vertical lines are locations of E_F from proton $(T_{1e}T)^{-1/2}$ parameters while dashed vertical line in (a) is predicted (Ref. 8) E_F position for fcc ZrH_2. $\Delta E(c/a)$ is energy difference between $N(E)$ maxima.

Although a quantitative determination of the energy difference $\Delta E(c/a)$ between the two maxima in $N(E)$ is beyond the capabilities of the present analysis, it is probably 1 eV or smaller. This value was estimated from the photoelectron spectra of Weaver, *et al.*[22] for $ZrH_{1.94}$ in which they observed a rather sharp peak in the d-band spectrum about 0.5 eV below their cutoff at E_F. Furthermore, the photoelectron spectra[22] for ϵ-phase ZrH_x are also consistent with E_F moving through a $N(E)$ peak. Because the instrumental resolution of the photoelectron spectra is about 0.4 eV, Weaver *et al.*[22] cannot detect an $N(E_F)$ peak until E_F lies more than about 0.4 eV above the peak. Hence, the sharp peak in Fermi-level emission spectra for $ZrH_{1.94}$ indicates E_F is a few tenths of an eV above a peak in $N(E)$ which is in qualitative agreement with the Fermi level for $ZrH_{1.94}$ predicted in Fig. 9(b). For $ZrH_{1.75}$, Weaver *et al.*[22] saw no indication of a peak in the Fermi-level emission of the photoelectron spectra while a small rise was observed for $ZrH_{1.88}$ as though E_F was near (or, just past) the middle of a peak which is being obscured by the instrumental resolution. These spectra suggest the $N(E)$ shape in Fig. 9(b) is at least qualitatively correct for ϵ-phase ZrH_x although the peak maximum and width cannot be reliably specified.

Further evidence in favor of the $N(E)$ distribution in Fig. 9(b) is provided by the electronic specific-heat measurements of Ducastelle *et al.*[11] and by the electron-spin-resonance studies[24] of 0.1 at.% Er substituted in ZrH_x. According to Ducastelle *et al.*[11] the $N(E_F)$ values for $ZrH_{1.55}$, $ZrH_{1.85}$, and $ZrH_{1.96}$ are 0.36, 0.76, and 0.46, respectively, in units of states/eV per metal atom. Hence, $N(E_F)$ is larger for the ϵ-phase ZrH_x samples than δ-phase $ZrH_{1.55}$ and the largest $N(E_F)$ occurs for ϵ-phase $ZrH_{1.85}$. This behavior is exactly as indicated in Fig. 9. Analyses[24] of the temperature-dependent increase in the linewidths of the Er ESR spectra for several ZrH_x samples also imply that $N(E_F)$ was substantially larger for the fct ϵ-phase compositions with a maximum near $x=1.85$–1.90. Thus, the $N(E)$ peak in Fig. 9(b) is again consistent with another independent experimental technique that monitors $N(E_F)$ behavior.

C. Comparison of electronic structures in TiH_x and ZrH_x

Although the TiH_x and ZrH_x systems have similar phase diagrams, crystal structures, and electronic properties, a number of qualitative and quantitative differences have been noted in Sec. II and in the literature.[5,8,11,15,16,21,22,48] For example, Table II compares the theoretical[8] partial density of states

TABLE II. Partial-wave analysis n_l of the density of electron states inside the muffin-tin metal and hydrogen spheres at the Fermi energy from APW calculations of Gupta and Burger (Ref. 8). $N_\uparrow(E_F)$ is the total density of states at E_F for one spin direction.

Sample	Site	n_s	n_p	n_d	n_f	$n_\uparrow(E_F)$
TiH_2	Ti	0.0015	0.0590	18.741	0.035	23.519
	1H	0.015	0.8755	0.0535	0.0015	
ZrH_2	Zr	0.004	0.073	10.805	0.035	16.460
	1H	0.008	0.432	0.021	0.001	

(n_l) at E_F for fcc TiH_2 and ZrH_2. The angular-momentum representation of n_l in Table II is relative to the local metal or hydrogen sites where the electron band structure is formed mainly from the hydrogen 1*s* orbitals and the metal *nd* and $(n+1)$ *s* orbitals. Thus, the n_p and n_f terms should not be considered to represent occupied *p* or *f* orbitals as an intra-atomic effect, but n_p and n_f at a given metal or hydrogen site primarily come from overlaps with the tails of the *d* orbitals from neighboring metal atoms.[8] Hence, the hyperfine interactions at the proton sites are due to local *s* states and the transferred core-polarization interactions with the *d* states on neighboring metal atoms as was presumed in Sec. V A. The dominant n_d value at the metal site and all the n_l values for the hydrogen sites are significantly larger for fcc TiH_2 to make the total $N(E_F)$ larger as well. This prediction is consistent with the various experimental results such as electronic specific heats[11] and magnetic susceptibilities[11,13,30,31] that are affected by $N(E_F)$. However, most of these experiments correspond to the fct phases for TiH_x and ZrH_x where $N(E_F)$ has already been decreased by the Jahn-Teller distortion, but the trend agrees with $N(E_F)$ values in Table II. The *s*-electron contributions at E_F are small at both the metal and hydrogen sites in TiH_2 and ZrH_2. However, n_s gives a significantly larger contribution at the hydrogen sites than at the metal sites, but n_s(H) is still less than 2% of the total partial n_l(H) in fcc TiH_2 and ZrH_2. The relative n_s(H) portion will probably be increased by the tetragonal distortion since the contributions from the metal *d* orbitals will be greatly reduced with only minor changes expected for the *s* band.

The proton $(T_{1e}T)^{-1/2}$ parameters of Göring *et al.*[26] for TiH_x and the present values for ZrH_x are compared in Fig. 10. If the proton hyperfine fields are assumed to be approximately equivalent for these systems, the proton $(T_{1e}T)^{-1/2}$ parameters in Fig. 10 imply the effective $N(E_F)$ values at the proton sites in ZrH_x are about 40% or less of the density of states at E_F in TiH_x. Taking the n_l values with $l \geq 1$ for the hydrogen sites from Table II, the ratio of the $N(E_F)$ in the fcc dihydrides is 0.49. The good agreement is consistent with the expected dominance of the $N_d(E_F)$ term in both hydrides and again indicates the n_s terms are not major contributors to the proton hyperfine interactions.[25,26] However, the n_s term can give a larger relative contribution in the fct TiH_x and ZrH_x phases since $N_d(E_F)$ is substantially decreased by the Jahn-Teller effect. The much larger tetragonal distortion in ZrH_x (i.e., a minimum c/a ratio of about 0.89 compared to a c/a ratio of about 0.945 in TiH_2 according to Yakel[48]) should yield a greater relative $N_d(E_F)$ difference between TiH_x and ZrH_x when $x \approx 2.00$, which is consistent with the $(T_{1e}T)^{-1/2}$ data in Fig. 10.

The Korringa parameters for the ZrH_x samples in Table I suggest a larger *s*-electron contact contribution than was apparent in similar analyses for $TiH_{0.99}$ and $TiH_{1.99}$ by Göring *et al.*[22] However, the actual difference cannot be reliably estimated considering the difficulty in accurately defining the absolute σ_K values in both studies, but a systematically

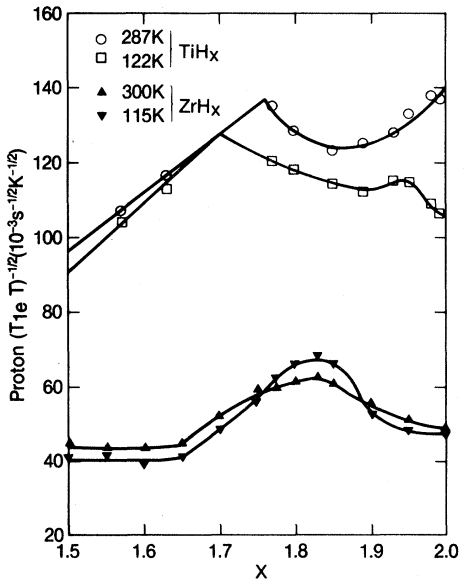

FIG. 10. Composition dependence of proton $(T_{1e}T)^{-1/2}$ for TiH_x (after Goring *et al.* in Ref. 26) and ZrH_x (present study).

larger n_s level for ZrH_x would not be unreasonable since the $N_d(E_F)$ value is also smaller in ZrH_x. Although Göring *et al.*[26] concluded that the tetragonal distortion reduced the relative population of t_{2d} d states at E_F, a similar evaluation for ϵ-phase ZrH_x is more difficult since the n_s and the various nonrigid-band-structure effects[1,8] cannot be readily identified for these samples and interpretation of the Korringa parameter q becomes much less straightforward. A partial density-of-states analysis in fcc TiH_2 by Fujimori and Tsuda[9] indicated the peak at E_F is due to the t_{2g} states. Assuming a similar situation in ZrH_2, the split peaks in Fig. 9(b) should also be primarily t_{2g} d bands sitting on top of smoothly varying e_g states. Hence, the largest t_{2g} contribution should be at the peak (i.e., near $ZrH_{1.83}$) and the smallest portion of t_{2g} states at $ZrH_{2.00}$. Unfortunately, the present g_{expt} values in Table I do not permit a clear assessment of the fraction of t_{2g} states for any of the ϵ-phase ZrH_x samples.

Some significant differences in the temperature behavior of the proton $(T_{1e}T)^{-1/2}$ values for TiH_x and ZrH_x are also indicated in Fig. 10. When $x \gtrsim 1.95$, $(T_{1e}T)^{-1/2}$ values for ZrH_x decrease with x and are nearly independent of temperature; whereas, the $(T_{1e}T)^{-1/2}$ values for TiH_x increase with x at 287 K and decrease with x at 122 K to produce an effective $N_d(E_F)$ reduction of nearly 25% for $TiH_{1.99}$ between these temperatures. This difference reflects the more rapid decrease[48] in the c/a ratio with decreasing temperature for the TiH_x system since the critical temperature is near 310 K while there will be only very minor variations in the ZrH_x c/a ratio which has already become nearly temperature independent[37,48] at these temperatures and compositions. Since the $N_d(E_F)$ decrease is predicted[1,4,7] to be proportional to the c/a ratio through the Jahn-Teller effect, the $N_d(E_F)$ in TiH_x will change rapidly[25,26] below 310 K but will be nearly constant for ϵ-phase ZrH_x when $x \geq 1.95$. $(T_{1e}T)^{-1/2}$ in the TiH_x system has only a positive temperature dependence, but a negative temperature dependence is observed for ZrH_x samples with $1.77 \leq x \leq 1.85$, which was related in the last section to E_F moving through a local maximum in the density of states with changes in hydrogen content. Although the $(T_{1e}T)^{-1/2}$ data in Fig. 10 suggest a peak in $N(E_F)$ may occur near $x \approx 1.75$ in TiH_x, it is clearly not of the same character as has been proposed for the $N(E)$ peak in the ZrH_x system. The Jahn-Teller distortion will definitely reduce $N(E_F)$ in TiH_x by a broadening of the sharp peak[7,9] at E_F, but the resulting splittings of the energy levels for the observed[48] 5% (or less) tetragonal distortion in TiH_x apparently cannot generate the resolved peaks proposed in Fig. 9(b) for ϵ-phase ZrH_x (where the tetragonal distortion exceeds 9% when $x \geq 1.75$). Hence, a continual $N(E_F)$ decrease is observed[25,26] in TiH_x with $x > 1.95$ as the temperature is lowered and the tetragonal distortion presumably becomes larger. Whether a similar distortion mechanism is also valid for TiH_x when $1.6 \leq x \leq 1.8$ will require further proton σ_K and T_1 measurements on additional samples as well as possible low-temperature x-ray diffraction measurements of the lattice parameters. However, the widely split $N(E)$ peaks in Fig. 9(b) are quite consistent with the behavior of the proton $(T_{1e}T)^{-1/2}$ and σ_K data in Fig. 8 as well as the other available experimental results[11,16,22,24] for ZrH_x. Band-theory calculations of the electronic structure of tetragonal (i.e., $c/a \approx 0.90$) $ZrH_{2.0}$ should provide a more quantitative verification of the split-band model represented in Fig. 9(b). Extensions of the existing calculations[1-9] to nonstoichiometric fcc and fct TiH_x and ZrH_x systems would be extremely helpful.

VI. CONCLUSIONS

Measurements of the proton spin-lattice relaxation times and Knight shifts in ZrH_x have indicated the dominance of a transferred core-polarization hyperfine interaction from the Zr d band to the s band at the hydrogen sites, which is completely analogous to the hyperfine interactions for protons in TiH_x (Refs. 25 and 26) and related ternary hydrides.[17,25] The ZrH_x band structure in the d-band region is significantly modified by the Jahn-Teller fct distortion when the hydrogen content exceeds $x = 1.75$. The predicted sharp peak at the Fermi level in fcc $ZrH_{2.0}$ is split into a resolved doublet in ϵ-phase ZrH_x with reduced densities of electron states as shown in Fig. 9. The composition and temperature dependences of the proton parameters $(T_{1e}T)^{-1/2}$ and σ_K indicate E_F will lie at different positions of the lower-energy peak as the hydrogen content in ϵ-phase ZrH_x is varied. Photoelectron spectra[22] and other experimental results[11,24] are consistent with this model.

ACKNOWLEDGMENTS

The support and advice of Dr. S. I. Chan is greatly appreciated. We thank Dr. W.-K. Rhim for providing the NMR spectrometer used to measure the Knight shifts. We also thank Dr. P. Richards for his helpful comments and suggestions. This work was supported by the California Institute of Technology President's Fund and Office of Basic Energy Sciences, Division of Chemical Sciences, U.S. Department of Energy. Mound is operated by the

Monsanto Research Corporation for the U.S. Department of Energy under Contract No. DE-AC04-76-DP00053. Sandia National Laboratories are supported by the U.S. Department of Energy under Contract No. DE-AC04-76-DP00789. This is Contribution No. 6685 from the A. A. Noyes Laboratory of Chemical Physics, California Institute of Technology.

---

*On leave from: Monsanto Research Corporation—Mound, Miamisburg, OH 45342.

[1]A. C. Switendick, J. Less-Common Metals 49, 283 (1976).

[2]A. C. Switendick, in *Transition Metal Hydrides—Advances in Chemistry Series 167,* edited by R. Bau, (American Chemical Society, Washington, D.C., 1978), p. 264.

[3]N. I. Kulikov, V. N. Borzunov, and A. D. Zvonkov, Phys. Status Solidi B 86, 83 (1978).

[4]N. I. Kulikov and V. N. Borzunov, Isv. Akad. Nauk. SSSR, Neorg. Mater. 14, 1292 (1978) [Inorg. Mater. (USSR) 14, 1292 (1978)].

[5]V. I. Savin, R. A. Andrievskii, V. I. Potorocha, and V. Ya. Markin, Isv. Akad. Nauk. SSSR, Neorg. Mater. 14, 1606 (1978) [Inorg. Mater. (USSR) 14, 1254 (1978)].

[6]M. I. Darby, M. N. Read, and K. N. R. Taylor, Phys. Status Solidi B 102, 413 (1980).

[7]M. Gupta, Solid State Commun. 29, 47 (1979).

[8]M. Gupta and J. P. Burger, Phys. Rev. B 24, 7099 (1981).

[9]A. Fujimori and N. Tsuda, Solid State Commun. 41, 491 (1982).

[10]R. C. Frisch and R. A. Forman, J. Chem. Phys. 48, 5187 (1968).

[11]F. Ducastelle, R. Caudron, and P. Costa, J. Phys. (Paris) 31, 57 (1970).

[12]E. F. Khodosov and N. A. Shepilov, Phys. Status Solidi B 49, K83 (1972); E. F. Khodosov and N. A. Shepilov, Fiz. Tverd. Tela. (Leningrad) 14, 939 (1972) [Sov. Phys.—Solid State 14, 807 (1972)].

[13]V. F. Nemchenko and V. G. Charnetskii, Isv. Akad. Nauk SSSR, Neorg. Mater. 10, 456 (1974) [Inorg. Mater. (USSR) 10, 392 (1974)].

[14]B. Nowak, N. Piślewski, and W. Leszczyński, Phys. Status Solidi A 37, 669 (1976).

[15]C. Korn, Phys. Rev. B 17, 1707 (1978).

[16]C. Korn, in *Hydrides for Energy Storage,* edited by A. F. Andresen and A. J. Maeland (Pergamon, Oxford, 1978), p. 119.

[17]B. Nowak, O. J. Żogal, and M. Minier, J. Phys. C 12, 4591 (1979).

[18]B. W. Veal, D. J. Lam, and D. G. Westlake, Phys. Rev. B 19, 2856 (1979).

[19]K. Tanada, N. Hamasaka, M. Yasuda, and Y. Fukai, Solid State Commun. 30, 173 (1979).

[20]K. R. Doolan, P. P. Narang, and J. M. Pope, J. Phys. F 10, 2073 (1980).

[21]J. M. Pope, P. P. Narang, and K. R. Doolan, J. Phys. Chem. Solids 42, 519 (1981).

[22]J. H. Weaver, D. J. Peterman, D. T. Peterson, and A. Franciosi, Phys. Rev. B 23, 1692 (1981).

[23]V. V. Nemoshkalendo, M. M. Kindrat, V. P. Krivitskii, B. P. Mamko, and A. I. Kharlamov, Isv. Akad. Nauk SSSR, Neorg. Mater. 17, 975 (1981) [Inorg. Mater. (USSR) 17, 699 (1981)].

[24]E. L. Venturini, Bull. Am. Phys. Soc. 26, 337 (1981); and unpublished.

[25]R. C. Bowman, Jr. and W.-K. Rhim, Phys. Rev. B 24, 2232 (1981).

[26]R. Göring, R. Lukas, and K. Bohmhammel, J. Phys. C 14, 5675 (1981).

[27]H. A. Jahn and E. Teller, Proc. R. Soc. London Ser. A 161, 220 (1937).

[28]A. C. Switendick, in *Hydrogen in Metals I: Basic Properties,* edited by G. Alefeld and J. Völkl (Springer, Berlin, 1978), p. 101.

[29]A. C. Switendick, Z. Phys. Chem. Neue Folge 117, 89 (1979).

[30]H. Nagel, and H. Goretzki, J. Phys. Chem. Solids 36, 431 (1975).

[31]H. Nagel and R. S. Perkins, Z. Mettalkd. 66, 362 (1975).

[32]B. Staliński and B. Nowak, Bull. Acad. Polon. Sci., Ser. Sci. Chim. 25, 65 (1977).

[33]A. Narath, in *Hyperfine Interactions,* edited by A. J. Freeman and R. B. Frankel (Academic, New York, 1967), p. 287.

[34]J. Winter, *Magnetic Resonance in Metals* (Clarendon, Oxford, 1971).

[35]G. C. Carter, L. H. Bennett, and D. J. Kahan, *Metallic Shifts in NMR* (Pergamon, Oxford, 1977).

[36]R. M. Cotts, in *Hydrogen in Metals I: Basic Properties,* Ref. 28, p. 227.

[37]R. L. Beck and W. M. Mueller, in *Metal Hydrides,* edited by W. M. Mueller, J. P. Blackledge, and G. G. Libowitz (Academic, New York, 1968), p. 241.

[38]P. W. Bickel and T. G. Berlincourt, Phys. Rev. B 2, 4807 (1970).

[39]K. G. Barraclough and C. J. Beevers, J. Nucl. Mater. 34, 125 (1970).

[40]S. Mishra, K. S. Sivaramakrishnan, and M. K. Asundi, J. Nucl. Mater. 45, 235 (1972/73).

[41]K. G. Barraclough and C. J. Beevers, J. Less-Common Metals 35, 177 (1974).

[42]S. S. Sidhu, N. S. Satya Murthy, F. P. Campos, and D. D. Zauberis, in *Nonstoichiometric Compounds-Advances in Chemical Series 39,* edited by R. Ward (American Chemical Society, Washington, D.C., 1963), p. 87.

[43]L. S. Topchyan, I. A. Naskidashvili, R. A. Andrievskii, and V. I. Savin, Fiz. Tverd. Tela. (Leningrad) 15, 2195 (1973) [Sov. Phys.—Solid State 15, 1461 (1974)].

[44]I. A. Naskidashvili, Yu. G. Sharimanov, N. Vilcu, D. Demco, and V. Simplaceanu, Fiz. Tverd. Tela (Leningrad) 19, 3465 (1977) [Sov. Phys.—Solid State 19, 2026 (1977)].

[45]I. N. Bydlinskaya, I. A. Naskidashvili, V. A. Melik-Shakhnazarov, and V. I. Savin, Fiz. Tverd. Tela (Leningrad) 22, 886 (1980) [Sov. Phys.—Solid State 22, 517 (1980)].

[46]V. F. Petrunin, V. P. Glazkov, V. I. Savin, V. A. Somenko, V. K. Fedotov, S. Sh. Shil'shteyn, and S. V. Marchenko, Fiz. Metal. Metalloved. 46, 206 (1978) [Phys. Met. Metallogr. (USSR) 46, 181 (1979)].

[47]R. C. Bowman, Jr., E. L. Venturini, and W.-K. Rhim, Phys. Rev. B 26, 2652 (1982).

[48]H. L. Yakel, Jr., Acta Crystallogr. 11, 46 (1958).

[49]W. L. Korst, USAEC Report NAA-SR-6880 (unpublished).

[50]MARZ-grade (i.e., stated purity of 99.99%) from Materials Research Corporation, Orangeburg, New York, 10962. Independent emission spectroscopy analysis at Mound has verified vendor claim of 20 ppm Fe and the absence of any detectable amount of other magnetic elements (e.g., Ni, Co, Mn, etc.).

[51]D. P. Burum, D. D. Elleman, and W.-K. Rhim, J. Chem. Phys. 68, 1164 (1978).

[52]P. Brill and J. Voitländer, Ber. Bunsenges. Phys. Chem. 77, 1097 (1973).

[53]S. Kazama and Y. Fukai, J. Less-Common Metals 53, 25 (1977).

[54]R. E. Taylor, T. Taki, and B. C. Gerstein, Phys. Rev. B 23, 5729 (1981).

[55]J. Mason, J. Chem. Soc. Dalton Trans. 1422 (1975).

[56]A. T. Nicol and R. W. Vaughan, J. Chem. Phys. 69, 5211 (1978).

[57]K. Terakura and J. Kanamori, J. Phys. Soc. Jpn. 34, 1520 (1973).

[58]N. Yokoyama, Y. Yamada, S. Kohzuki, and K. Asayama, J. Phys. Soc. Jpn. 37, 73 (1974).

[59]A. V. Skripov and A. P. Stepanov, Fiz. Tverd. Tela (Leningrad) 23, 966 (1981) [Sov. Phys.—Solid State 23, 560 (1981)].

[60]J. Kanamori, H. K. Yoshida, and K. Terakura, Hyperfine Interact. 9, 363 (1981).

[61]B. Stalinski, C. K. Coogan, and H. S. Gutowsky, J. Chem. Phys. 34, 1191 (1961).

[62]J. Korringa, Physica 16, 601 (1950).

[63]Y. Yafet and V. Jaccarino, Phys. Rev. 133, A1630 (1964).